# Structures and Transport Properties of
Hydrated Water-Soluble Dendrimer-Grafted Polymer Membranes
for Application to Polymer Electrolyte Membrane Fuel Cells

Seung Soon Jang[*] and William A. Goddard III[**]

Materials and Process Simulation Center (MC 139-74)

California Institute of Technology, Pasadena, CA 91125

1. Introduction

Enormous efforts have been and continue to be expended toward developing improved polymer electrolyte materials for polymer electrolyte membrane fuel cell (PEMFC).[1-6] This has led to a number of new materials, but Nafion continues to be considered as the material of choice due to its high proton conductivity (0.1 S/cm at 80 ℃ and 100% RH) and its excellent chemical and thermal stability.[7-11] Even so there continues to be a need to find alternative materials that can perform well at higher temperatures (120 ℃ or above).

Recently we proposed a strategy for improving the performance of PEMFC by utilizing a dendritic molecular architecture having the following favorable features:[12] i) a well controlled nanoscale segregation of the hydrophilic acid containing regions arising from the monodisperse molecular weight distribution achievable by the stepwise iterative synthetic route used for dendrimers; ii) the controllability of the distribution of the terminal acid groups at the periphery (or surface) of the dendrimer by the specific choices in the monomers from which the dendrimer is constructed. We considered that this direct control over the spacing in the hydrophilic regions could allow designs in which the water solvent could be retained in the membrane at temperatures above 100 ℃. Our previous studies on the Dendrion made a very simple choice for the hydrophobic polymer backbone to which the dendrimer is attached. Now we want to consider the issue of the optimum choice of the polymer backbone. An advantage of the Dendrion concept is that that the dendrimer controls the sizes of the hydrophilic domains independently of the nature of the polymer backbone, which determines the spatial distribution of these hydrophilic domains and the nature of the hydrophobic domains. In contrast, for Nafion the nanophase distribution of hydrophilic and hydrophobic domains and the positioning of the acid groups within these domains is a complex function of the branching and monomers of the polymer backbone.
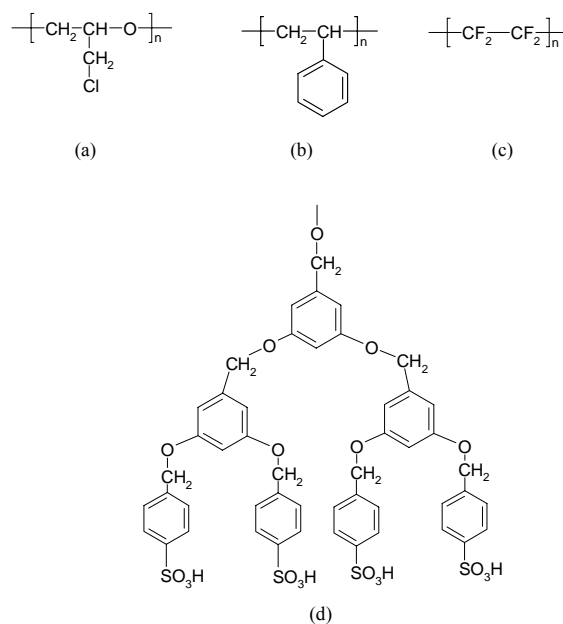
Figure 1. Chemical structures of backbone polymers and dendrimer; (a) poly (epichlorohydrin), PECH; (b) poly (styrene), PS; (c) poly (tetrafluoroethylene), PTFE; (d) the second generation poly aryl ether dendrimer with four sulfonic acid groups.

[*] jsshys@wag.caltech.edu

[**] To whom correspondence should be addressed. wag@wag.caltech.edu

Thus we consider here three different types of linear backbone polymers such as poly (epichlorohydrin) (PECH, Figure 1a), poly (styrene) (PS, Figure 1b), and poly (tetrafluoroethylene) (PTFE, Figure 1c), to each of which the same the water-soluble dendrimer is grafted as shown in Figure 2.

In order to assess how the nanophase-segregation and transport in hydrated membrane depend on the type of backbone polymer, we predict the membrane structure consisting of dendrimer-grafted polymers with 10 and 20 wt % of water content. The results for these dendrimer-grafted polymer systems are compared with the properties of Nafion membrane and Dendrion membrane calculated using the same simulation techniques.[12,13]

(a) PECH-D2 (EW=652)

(b) PS-D2 (EW=633)

(c) PTFE-D2 (EW=661)

Figure 2. Full atomistic models of the second generation polyaryl ether dendrimer-grafted polymers. The number of dendrimer per chain is the same for all cases and the values in the parenthesis denotes the equivalent weight for each polymer. The conformations in the right-hand side are equilibrated ones from their hydrated membranes.

2. Simulation Details

All simulations were carried out using a full-atomistic model of the second-generation polyaryl ether dendrimer-grafted copolymers as shown in Figure 2. The degree of polymerization of each backbone polymer was determined to have an equivalent weight of ~650.

We used the DREIDING force field[14] as previously used to study Nafion[13,15-18] and Dendrion[12] except that the fluorocarbon parts were described using recently optimized force field[19] parameters and the water was described using the F3C force field.[20] These force field parameters are described in the original papers[14,19,20] and in our previous study[13] on hydrated Nafion. Thus the force field has the form:
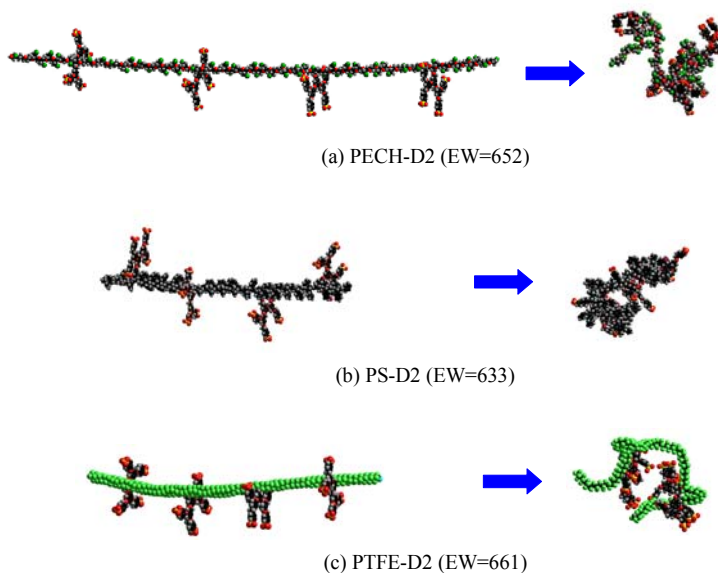
$$E_{total} = E_{vdW} + E_Q + E_{bond} + E_{angle} + E_{torsion} + E_{inversion} \qquad (1)$$

where E_{total}, E_{vdW}, E_Q, E_{bond}, E_{angle}, $E_{torsion}$ and $E_{inversion}$ are the total energies and the van der Waals, electrostatic, bond stretching, angle bending, torsion and inversion components, respectively.

The individual atomic charges of the copolymer were assigned using the charge equilibration (QEq) method[21] optimized to reproduce Mulliken charges of small molecules. The atomic charges of water molecule were from the F3C water model.[20] The Particle-Particle Particle-Mesh (PPPM) method[22] was used to calculate the electrostatic interactions.

All the annealing and MD simulations were performed using the MD code LAMMPS (Large-scale Atomic/Molecular Massively Parallel Simulator) from Plimpton at Sandia[23,24] with modifications to handle our force fields.[12,13,25] The equations of motion were integrated using the velocity Verlet algorithm[26] with a time step of 1.0 fs. The Nose-Hoover temperature thermostat for the NVT and NPT MD simulations used the damping relaxation time of 0.1 ps and the dimensionless cell mass factor of 1.0.

We constructed hydrated membrane systems for each kind of backbone polymer using two water concentrations of 10 wt % and 20 wt % as summarized in Table 1. We expect that all of the 48 sulfonic acid groups in the membrane to be ionized. To provide a measure of the statistical uncertainties, all data in this paper were obtained from two independent samples for each backbone polymer with 10 wt % and 20 wt % of water content using different initial configurations.

2

Table 1. Composition and densities of simulated hydrated dendrimer-grafted copolymer

	PECH-D2		PS-D2		PTFE-D2	
Molecular weight	10430		10130		10614	
Equivalent weight	652		633		661	
No. of sulfonate group			48			
No. of chain			3			
Temperature (K)			353.15			
No. of Water (H_2O/SO_3H)	240 (5)	480 (10)	240 (5)	480 (10)	240 (5)	480 (10)
Water content (wt %)	10	20	10	20	10	20
Density (g/cm^3)	1.22±0.01	1.22±0.01	0.98±0.01	1.06±0.01	1.49±0.01	1.42±0.01
Volume (Å^3)	49730±360	55960±280	61270±440	63000±380	38870±280	45790±340

In addition to the simulations described above, we constructed 8-times-larger systems by making 2×2×2 superstructure of the smaller systems and implemented independent simulations to investigate the characteristic dimension of phase-segregation and to analyze characteristic dimensions. These larger scale calculations used 24 dendrimer-grafted polymer chains and 3840 water molecules in the simulation cell for 20 wt % of water content. However, the dynamical properties (e.g., diffusion) reported here are based on the smaller system.

The time scales for relaxation of polymers is extremely slow, far too slow for standard equilibrium MD to evolve to the equilibrium structure. In order to obtain well equilibrated structures for complex amorphous polymers with a minimum of effort, we have developed a general annealing procedure, which accelerates the attainment of equilibrium by driving the system repeated through cycles of thermal annealing and pressure annealing. This procedure aims to help the system to quickly escape from various local minimum to find the globally better structures and for heterogeneous systems it promote the migration of species required for optimum phase-segregation. This annealing equilibration procedure was used in exactly the same way in our previous studies of Nafion[13] and Dendrion.[39] This annealing procedure achieves a fully equilibrated system at the target temperature and pressure. We emphasize here that we do *not* bias the predicted structure by imposing any particular geometry (cylinders, spheres, lamellae) for the distribution of water in the system, nor do we impose any particular density or packing. Rather the strategy of temperature and pressure MD annealing is designed to obtain an equilibrated distribution of water in an equilibrated polymer system at target conditions (in this case 353.15 K and 1 atm). This led to a final density of each dendrimer-grafted polymer as summarized in Table 1.

After completing step g of the annealing, we equilibrated the system using NPT MD simulations for *another 5 ns* at 353.15 K for use in calculating properties. This is the operating temperature of Nafion-based PEMFC was used in our previous simulations, allowing us to compare the properties of the dendrimer-grafted polymer directly with those of the Nafion and the Dendrion.

3. Results and Discussion

Figure 3 presents snapshots of the final frame from the NPT MD simulations which show that
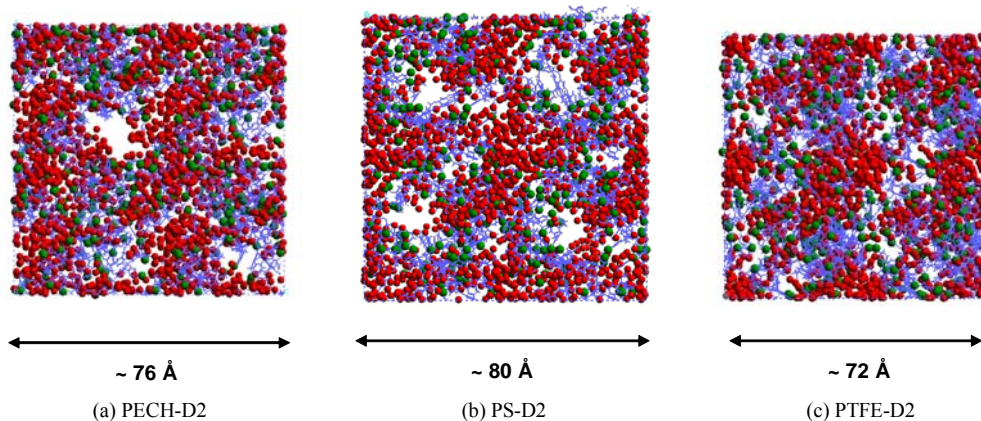
Figure 3. Nanophase-segregated structures of the hydrated dendrimer-grafted copolymer membrane with 20 wt % water content predicted from the simulations at 353.15 K. Blue components denote dendrimer and Green balls denote the sulfur atoms and Red balls denote the oxygen atoms of water molecules. For clarity, the backbone polymer chains are not shown.
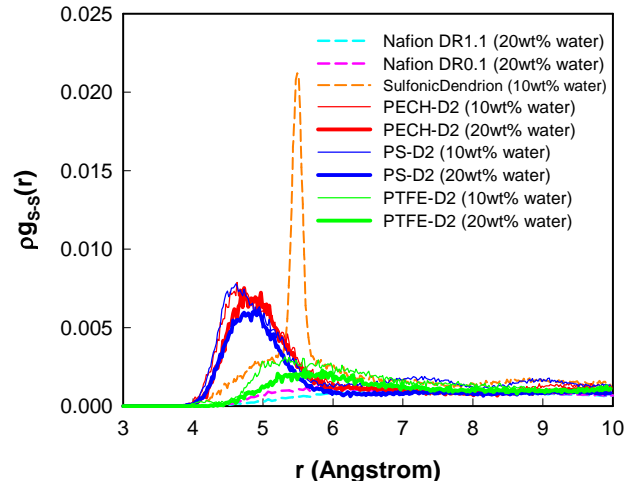
water molecules are well associated with the water-soluble dendrimer and form water phase. A noticeable difference is observed among PECH-D2, PS-D2, and PTFE-D2 with respect to the structure and dimension of the hydrated membrane. These differences seem to be strongly influenced by the type of backbone polymer even under the same conditions in terms of molecular weight, equivalent weight, and water content. This shows that the nature of the polymer backbone affects both the packing of backbone and the spacing of the dendritic regions. This section analyzes the properties of the membrane and compares the affects of each type of backbone polymer.
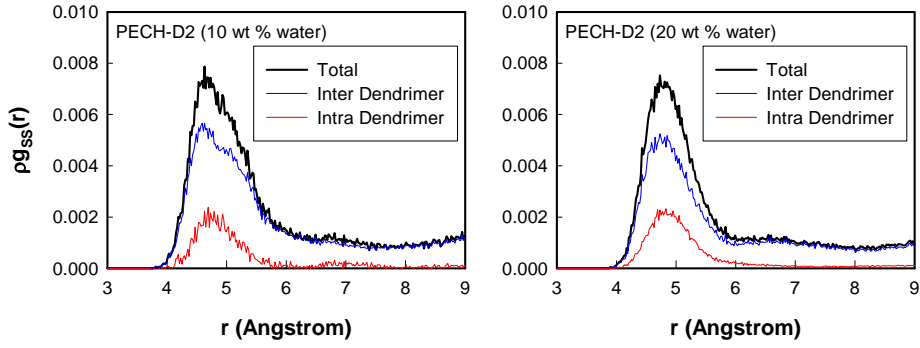
3.1 Correlations of Acid Group

Figure 4 shows the pair correlation functions for sulfur-sulfur pairs, $g_{S-S}(r)$. This pair correlation function, $g_{A-B}(r)$ indicates the probability density of finding A and B atoms at a distance r, averaged over the equilibrium trajectory as defined by

$$g_{A-B}(r) = \left(\frac{n_B}{4\pi r^2 dr}\right) / \left(\frac{N_B}{V}\right)$$

where n_B is the number of particle B located at the distance r in a shell of thickness dr from particle A, N_B is the number of B particles in the system, and V is the total volume of the system.
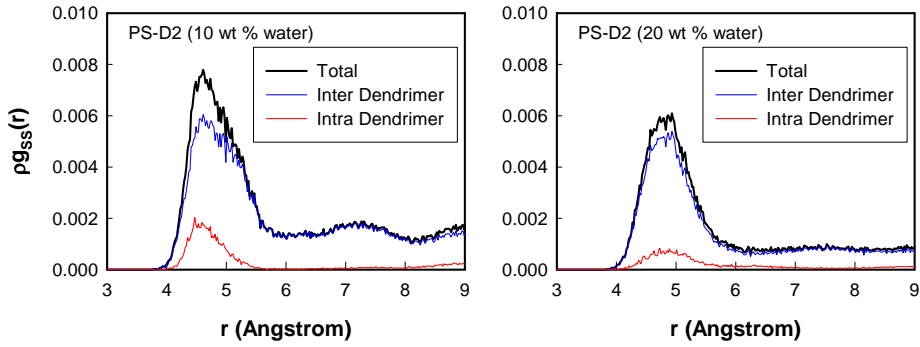
This pair correlation analysis (Figure 4), shows a maxima of PECH-D2(g_{S-S}= 4.7 Å for 10 wt % H_2O and g_{S-S}= 4.9 Å for 20 wt % H_2O); PS-D2 (g_{S-S}= 4.7 Å for 10 wt % H_2O and g_{S-S}= 4.9 Å for 20 wt % H_2O) with a similar distributions of sulfonic acid groups and

Figure 4. Pair correlation function of sulfonic acid group in the hydrated membranes. The $g_{S-S}(r)$ for Nafion and Dendrion was reported previously.[12,13] ρ indicates the number density of sulfur.

almost the same peak position for both of water content. This is a much closer S-S distance than that observed in our previous simulations: Nafion (6~7 Å) for 20 wt % H_2O [13] and Dendrion (5.5 Å) for 10 wt % H_2O.[12] In contrast, for PTFE-D2 we found PTFE-D2 (g_{S-S}= 5.3 Å for 10 wt % H_2O and g_{S-S}= 5.6 Å for 20 wt % H_2O) which is larger than PECH-D2 and PS-D2.

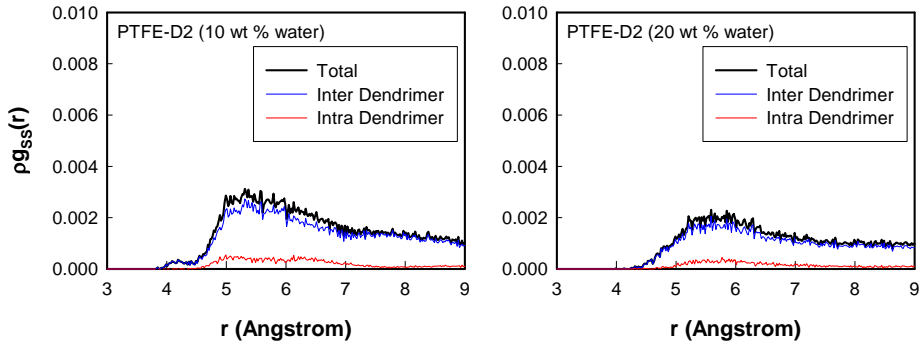**Figure 5.** Decomposition of pair correlation function of acid group. "Inter Dendrimer" denotes the contribution from the pair of sulfonic acid groups belonging to different dendrimers whereas "Intra Dendrimer" from the pair of sulfonic acid groups belonging to the same dendrimer.

The overall distribution of S-S distances for PTFE-D2 is much broader than for PECH-D2 and PS-D2. To understand the origin of this difference we decomposed the total $\rho g_{S-S}(r)$ into the contribution from acid pairs belonging to the same dendrimer (*intra dendrimer*) and the contribution from acid pairs belonging to different dendrimers (*inter dendrimer*) as shown in Figure 5. Here we see that the PECH-D2 (Figure 5a) and the PS-D2 (Figure 5b) have more *intra dendrimer* contributions for S-S

distance < 5 Å than for PTFE-D2 (Figure 5c).

From this decomposition of $\rho g_{S-S}(r)$ in Figure 5, we found that the dominant correlation distance between sulfonate groups is nearly the same for both inter dendrimer and intra dendrimer, indicating that the dendrimers are in sufficiently close contact with each other and that the sulfonic acid distributions are uniform. We expect that this characteristic would help the membrane retain a continuous hydrophilic water phase in the nanophase-segregated morphology providing efficient the proton transfer rates. To clarify this point, Figure 6 shows connections between sulfur atoms of sulfonate groups within 7 Å distance of each other, This shows a well-interconnected sulfur network for all cases, indicating that *dendrimers contact each other to form a percolated structure.*


| ~ 76 Å | ~ 80 Å | ~ 72 Å |
| (a) PECH-D2 | (b) PS-D2 | (c) PTFE-D2 |
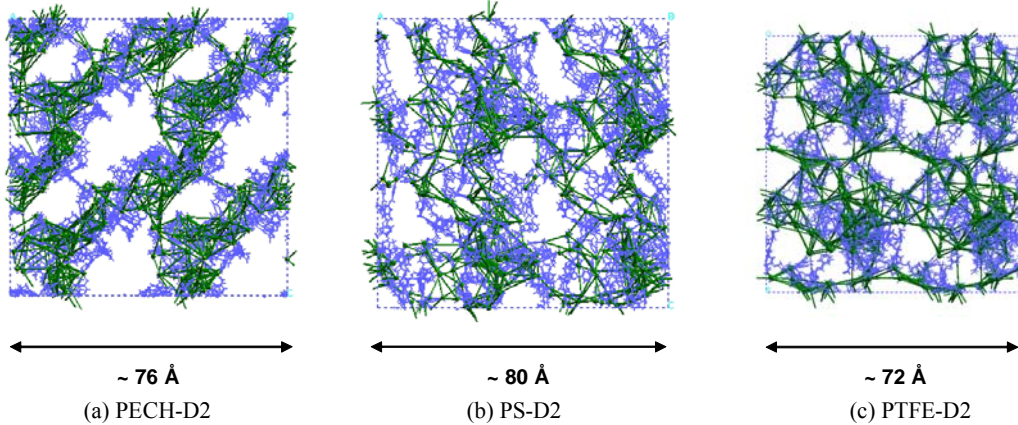
Figure 6. Distribution of sulfurs in sulfonic acids with 20 wt% of water content. The bonds are generated between sulfur atoms within 7 Å.

Figure 5 shows that $\rho g_{S-S}(r)$ is not significantly affected by the water content. Thus increasing the water content by 100 % increases the average S-S distance by 4% (0.2~0.3 Å). As discussed previously,[12] we believe that this insensitivity of $\rho g_{S-S}(r)$ to the water content results from the structural characteristics of the dendrimer in which the terminal sulfonate groups are locally concentrated through covalent connectivity in a well-defined structure. We consider this to be a positive aspect in retaining a constant structure during the fuel cell operation which may undergo a significant fluctuation in water content.

3.2 Structure of the Water in the Membrane

The characteristics of the water phase in the hydrated membrane are most important to the fuel cell performance since the proton transfer occurs through the water phase. Extensive studies on the proton transfer in water[27-36] and in polymer electrolyte membranes,[3,29-31,37-39] have led to the general consensus that the proton diffusion rate in bulk water is 4~8 times larger than in the hydrated membrane. As summarized by Kreuer[29,31] and by Paddison,[3] this is attributed to the bulk water having a well-organized and compact hydrogen bonding network that aids efficient proton hopping. In contrast the hydrated membranes has a reduced hydrogen bond connectivity. Especially, Paul and Paddison described this aspect from the viewpoint of dielectric saturation of water by analyzing the
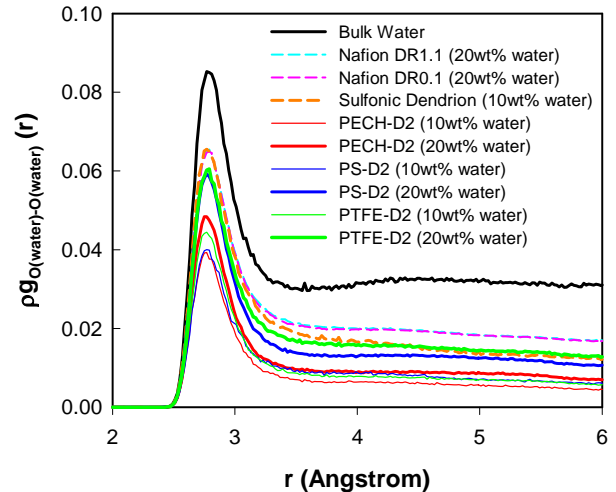
Figure 7. Product of pair correlation functions of water oxygens, $g_{O(water)-O(water)}(r)$ with water number density (ρ).

6

restricted dynamics of water dipole moment in vicinity of anionic groups through their molecular statistical mechanical model.[40]

In order to characterize the structure in the water phase dispersed within a hydrated membrane, we calculated $\rho g_{O(water)-O(water)}(r)$ (see Figure 7). For comparison, the cases of bulk water and the results from our previous studies on the Nafion and the Dendrion are also included here. For the bulk water phase we calculated a water coordination number of $CN_{H2O}=4.59$, in very good agreement with the value of $CN_{H2O}=4.5$ computed from neutron diffraction experiments.[41] We also calculated the average water coordination number for water for all cases simulated in this study as summarized in Table 2. For the Dendrimer-grafted polymers PECH-D2 ($CN_{H2O}=1.75$ for 10 wt % H2O and $CN_{H2O}=2.37$ for 20 wt % H2O); PS-D2 ($CN_{H2O}=1.92$ for 10 wt % H2O and $CN_{H2O}=2.97$ for 20 wt % H2O); PTFE-D2 ($CN_{H2O}=2.01$ for 10 wt % H2O and $CN_{H2O}=3.16$ for 20 wt % H2O). Obviously, the structure of the water phase in the membranes approaches a bulk-water-like structure with increasing water content.

Table 2. Water coordination number for water in membrane

System		Water content (wt %)	Water coordination number
Bulk water		—	4.59 (exp. 4.5)
PECH-D2		10	1.75
		20	2.37
PS-D2		10	1.92
		20	2.97
PTFE-D2		10	2.01
		20	3.16
Nafion	dispersed DR=1.1	20	3.85 [a,b]
	blocky DR=0.1	20	3.82 [a,b]
Sulfonic Dendrion		10	3.40 [b]

a Reference [12,13]; b Reference [12,13]

Of course the structure of the water phase is affected by the type of backbone polymer. Thus the attractive interactions of water with a hydrophilic backbone polymer may perturb the structure in water phase more than does a hydrophobic backbone (for a given water content) because water molecules can associate more strongly with hydrophilic backbone polymers in comparison with hydrophobic ones. Since the three types of dendrimer-grafted polymer membrane were simulated under the same conditions including equivalent weight, dendrimer structure, water content, and temperature. We may infer that the structural difference in water phase observed in our simulations is attributed to the difference in the interaction between water and backbone polymer. Indeed Figure 8 shows that the attractive interaction of backbone polymer with water molecules decreases in order of PECH-D2 > PS-D2 > PTFE-D2 for both water contents. We attribute this relatively more attractive interaction of PECH-D2 backbone with water to the hydrophilicity of epichlorohydrin (the monomeric unit of PECH-D2 backbone). Thus the hydrophilic PECH can absorb a certain amount of water even without a hydrophilic dendrimer, as shown experiment.[42]
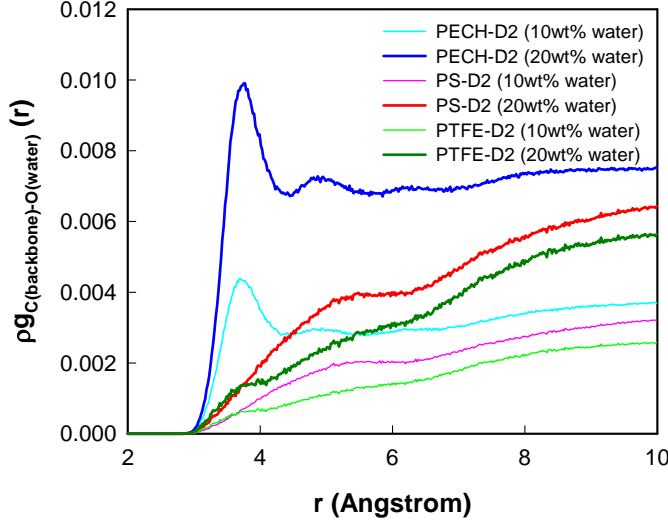
Figure 8. Product of pair correlation functions of carbon in backbone polymer and water oxygen, $g_{C(backbone)-O(water)}(r)$ with water number density (ρ).

However the results in Table 2 raise the question as to why the water coordination numbers of water in the dendrimer-grafted polymers are smaller than those in the Nafion (3.82~3.85) and the sulfonic Dendrion (3.40). Thus even though PTFE-D2 has exactly the same kind of backbone polymer (PTFE) used in the Nafion and the Dendrion, the water coordination number of water for the PTFE-D2 is smaller than that for the Nafion (3.16 for the PTFE-D2 and 3.82~3.85 for the Nafion at 20 wt% water content,; and 2.01 for the PTFE-D2 and 3.40 for the sulfonic Dendrion at 10 wt% water content,). At least part of the explanation is that the equivalent weight for PTFE-D2 (~660) is about half that for the Nafion and the Dendrion (~1200). Thus, the PTFE-D2 has higher sulfonic acid group density than the other two, making it plausible that the structure in water phase for the PTFE-D2 is perturbed more by the nearly two-fold greater number of strong acid groups in the membrane.
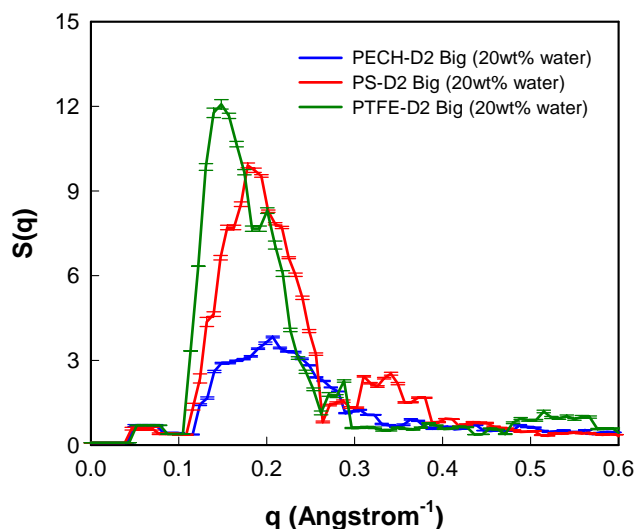
3.3 Structure Factors

The differential backbone polymer-water interactions discussed above should be reflected in the phase-segregation of dendrimer-grafted polymer membrane. To provide a quantitative measure of the extent of nanophase-segregation that can in principle be extracted from experiment, we calculated the structure factor, $S(q)$ that would be observed in small angle scattering experiments (SAXS and SANS),

using $S(\mathbf{q}) = \left\langle \sum_{r_i} \sum_{r_j} exp(i\mathbf{q} \cdot \mathbf{r}_{ij})(\xi^i \xi^j - \langle \xi \rangle^2) \right\rangle / L^3$ where the angular bracket denotes a thermal statistical

average, ξ^i represents a local density contrast, $(\phi_A^j - \phi_B^j)$, $\mathbf{q}$ is the scattering vector and $\mathbf{r}_{ij}$ is the vector between the sites i and j. This analysis has been used successfully to investigate the phase-segregation in our previous studies on the hydrated membrane for the Nafion[13] and the Dendrion.[12] The SAXS experiments measure the electron density contrast and while SANS experiments measure deuterium density contrast. For our analysis we assigned an artificial density contrast as follows. The local density variables are ϕ_A^j is equal to 1 if the site j is occupied by a hydrophilic entity such as water or an acid group and equal to 0 otherwise, and ϕ_B^j is equal to 1 if the site is occupied by hydrophobic entities such as PTFE backbone and equal to zero otherwise. The quantity $S(\mathbf{q})$ is spherically averaged as $S(q) = \sum_{|\mathbf{q}|} S(\mathbf{q}) / \sum_{|\mathbf{q}|} 1$ ($q = (2\pi / L)n$) where $n = 1, 2, 3, \cdots$ denotes that, for a given n, a spherical shell is taken as $n - 1/2 \le qL/2\pi \le n + 1/2$.

Our previous studies for the hydrated Nafion membrane[13] led to a characteristic dimension of nanophase-segregation of ~ 30 for a dispersed monomeric sequence and ~ 50 Å for a blocky monomeric sequence. Similar studies for the hydrated PTFE Dendrion membrane.[12] led to ~30 Å. For the hydrated dendrimer-grafted polymer membranes, we found the structure factor profiles as a function of scattering vector, **q,** shown in Figure 9. These structure factor profiles were calculated for the *large* system

Figure 9. Structure factor profile for hydrated dendrimer-grafted polymer membrane with 20 wt % of water content simulated at 353.15 K. This shows that the characteristic dimension of nanophase segregated structure is ~20 Å (q= ~0.20 Å^{-1}), ~35 Å (q= ~0.18 Å^{-1}) and ~40 Å (q= ~0.15 Å^{-1}) for PECH-D2, PS-D2 and PTFE-D2, respectively.

consisting of 24 polymer chains as mentioned in section 2. This is because the small system consisting of 3 polymer chains would not allow the structural development of the phase-segregation beyond its system size (36 ~ 40 Å corresponding to q=0.15 ~ 0.17 Å^{-1}).

At 20wt% water content the structure factor analysis in Figure 9 leads to a maximum intensity at ~0.20 Å^{-1} for PECH-D2, corresponding to the characteristic dimension of ~20 Å; ~ 0.18 Å^{-1} for PS-D2, corresponding to the characteristic dimension of ~35 Å; ~0.15 Å^{-1} for PTFE-D2, corresponding to the characteristic dimension of ~40 Å. In addition the intensity of these peaks (indicating the density contrast between hydrophobic domain and water domain) increases in order of PECH-D2 < PS-D2 < PTFE-D2. From these observations, we conclude that the dimensions of the nanophase-segregation is in the order of PECH-D2 < PS-D2 < PTFE-D2. This result from structure factor analysis is very consistent with the analyses (Figures 3, 7 and 8) in previous sections: a more hydrophobic backbone polymer leads to a larger extent of nanophase-segregation in the membrane, making the structure in water phase closer to the bulk water.

3.4 Diffusion of Water in the Membrane

Most critical to the performance of PEMFC is the proton conductivity (which we want to be large) and the water diffusion. The proton conductivity is especially dependent on the rotational dynamics of water molecules to facilitate a continuously evolving proton hopping. Although the role of water rotation in the hydrated membrane is essential for a fundamental understanding of proton conduction, it has been little analyzed. Probably this is due to the lack of experimental tools capable of directly measuring this phenomenon in the membrane. Here we analyze the rotational water dynamics in the hydrated dendrimer-grafted polymer membrane and compare it with the values computed and measured for bulk water.

A second important feature of water dynamics in hydrated membrane is the translational diffusion coefficient. If the membrane possesses a high electro-osmotic drag coefficient, it may be necessary to have a high translational diffusion value for water to regulate a uniform water distribution by concentration-gradient driven drift toward the anode. Inversely, we expect that the electro-osmotic drag of water by the protons would be difficult in an environment having low translational mobility of water. An example is the ice near the melting point where the translational diffusion of water is strongly restricted while the rotational degree of freedom is active.

Previously[12,13] we showed that the membrane transport properties depend on the extent of nanophase-segregation between hydrophilic and hydrophobic phase, in agreement with experimental observations.[2,6,31,43] For PEMFC applications, we want to minimize water mobility in order to reduce the electro-osmotic drag of water as protons are transported from anode to cathode. Otherwise the membrane near the anode can become too dry while the membrane near the cathode floods, producing uneven and unpredictable changes in the conductivity of the membrane during operation of the cell. Thus, we prefer that water in the membrane have a bulk-water-like water phase that percolates throughout the membrane to aid proton transport while simultaneously minimizing translational transport. In this section, we analyze water dynamics from the 5ns NPT MD simulation in terms of the rotational and translational diffusion.

3.4.1 Rotational diffusions

9

To determine the rotational dynamics of water, we calculated the rotational diffusion coefficient (D_R) as[44] $D_R = \dfrac{kTS(0)}{12N}$ where k is the Boltzmann constant, T is absolute temperature, N is the number of water molecules. S(0) is the rotational density of states at zero frequency $S(\upsilon)\big]_{\upsilon=0} = \dfrac{2}{kT} \lim_{\tau-\infty} \int_{-\tau}^{\tau} C_R(t)e^{-i2\pi\upsilon t}dt\bigg]_{\upsilon=0}$. Here $C_R(t)$ is the autocorrelation function of angular velocity, $\omega_{ij}^{CM}(t)$ of water molecule (i) $C_R(t) = \sum_{j=1}^{3} c_{R_j}(t) = \sum_{i=1}^{n}\sum_{j=1}^{3} <\omega_{ij}^{CM}(t)\omega_{ij}^{CM}(0)>$. This analysis allows us to evaluate the rotational diffusion of water molecules in this dendrimer-grafted polymer membrane.

Table 3. Rotational diffusion coefficients (D_R) of water from the MD simulations. This is expected to correlate with proton transport rates.

System			D_R (×10^{11} /s)	
			T=298.15 K	T=353.15 K
Bulk water			3.25±0.24[c] (exp. 2.2[a])	7.05±0.42[c]
PECH-D2	10 wt % water content			2.66±0.31
	20 wt % water content			3.58±0.33
PS-D2	10 wt % water content			4.44±0.32
	20 wt % water content			5.70±0.33
PTFE-D2	10 wt % water content			4.70±0.30
	20 wt % water content			6.10±0.31
Nafion	dispersed DR=1.1	20 wt % water content		7.42±0.54[b,c]
	blocky DR=0.1	20 wt % water content		6.23±0.53[b,c]
Sulfonic Dendrion	10 wt % water content			7.49±0.45[c]

a Reference [45]; b Reference [13]; c Reference [12].

As summarized in Table 3, the calculated rotational diffusion rate (D_R) for bulk water of (3.25±0.24)×10^{11}/s, which is comparable to the experimental value[45] of 2.2×10^{11}/s at the same temperature of 298.15 K. For the higher temperature of 353.15 K we predict that the D_R of bulk increases by a factor of 2.2 (to 7.05±0.42×10^{11}/s) (we have not found experimental data at this higher temperature).

Table 3 shows that the D_R of water in the dendrimer-grafted polymer membrane increases with increasing water content for all cases in this study. As discussed in section 3.2, the water phase in the hydrated membrane is associated with the strong acid groups of dendrimers to solvate, and the rotation of water molecules that solvate the strong acid groups should be restricted due to the charge-dipole interaction between strong acid group and solvating water molecules. Considering that the system with higher water content has more water molecules not involved directly in solvating strong acid groups in

comparison to that with lower water content, it seems reasonable that the system with higher water content has a larger value of D_R than that with lower water content. Moreover, this explanation also implies that as the water content increases, the structure in water phase approaches that in bulk water since the portion of solvating water decreases in that water phase.

We find that the D_R of water increases in order of PECH-D2 < PS-D2 < PTFE-D2 at the same water content. We attribute this result to the difference in the nanophase-segregation for each backbone polymer: the larger the scale of the nanophase-segregation, the closer the structure in water phase approaches that in bulk water, and thereby the closer the water rotation in the water phase of membrane approaches that in bulk water. This result is consistent with our previous discussions in sections 3.2 and 3.3.

On the other hand, comparison with our previous results from Nafion (D_R =6.2~7.4×10^{11}/s)[13] and Dendrion (D_R =7.5×10^{11}/s)[12] (Table 3), only the PTFE-D2 membrane with 20 wt% of water content shows a comparable value, D_R = 6.10×10^{11}/s. The other 5 cases have smaller values. As discussed in section 3.2, we believe that this is due to the smaller equivalent weight of dendrimer-grafted polymers. The increased concentration of sulfonic acid groups in the water phase perturbs the structure of the water phase, making more different from bulk water. The consequence is that the water rotation decreases, in consistency with the studies by Paddison and his coworkers [40,46,47]

3.4.2 Translational diffusions

This analysis of the translational diffusion of water, finds the same trend as observed in previous sections: the higher the water content in the membrane, the closer translational diffusion of water to that of bulk water.

Table 4. Translational diffusion coefficients (D_T) of water from the MD simulations.

System			D_T (×10^5 cm^2/s)	
			T=298.15 K	T=353.15 K
Bulk water			2.69±0.04 (exp. 2.30[a])	5.98±0.07 (exp. 6.48[a])
PECH-D2	10 wt % water content			0.05±0.03
	20 wt % water content			0.23±0.04
PS-D2	10 wt % water content			0.10±0.04
	20 wt % water content			0.43±0.04
PTFE-D2	10 wt % water content			0.16±0.04
	20 wt % water content			0.57±0.04
Nafion	DR=1.1	20 wt % water content		1.43±0.07[b] (1.25[c])
	DR=0.1	20 wt % water content		1.62±0.05[b] (1.25[c])
Sulfonic Dendrion	10 wt % water content			0.37±0.06[b,d]

a Reference [48-50]; b Reference [13]; c Reference [51]; d Reference [12].

The translational diffusion coefficients (D_T) of water is obtained using $\left\langle (r(t) - r(0))^2 \right\rangle = 6 D_T t$ with the linear part of the MSD, as our previous studies.[12,13] These values are summarized in Table 4 which shows

that for all cases, the D_T of water increases with increasing water content. The calculated values in bulk water are $D_T = (2.69\pm0.04)\times10^{-5}$ cm^2/s at 298.15 K and $(5.98\pm0.07)\times10^{-5}$ cm^2/s at 353.15 K, which agrees reasonably well with the experimental values ($D_T = 2.30\times10^{-5}$ cm^2/s at 298.15 K and 6.48×10^{-5} cm^2/s at 353.15 K).[48-50]

We find that for the same water content D_T increases in order of PECH-D2 < PS-D2 < PTFE-D2 which is the same trend as the scale of nanophase-segregation, which is also consistent with the results in the previous sections.

In addition, we compare the D_T of water in the dendrimer-grafted polymer membrane with those in the Nafion and the Dendrion membrane. All of the membranes simulated in this study have a smaller D_T than Nafion and Dendrion at the same water content, which suggests that they may have reduced the electro-osmotic drag coefficient. As discussed in our previous study on the hydrated Dendrion membrane,[12] the inner structure of hydrophilic dendrimer architecture may work efficiently in reducing the translational mobility of water while retaining the level of its rotational mobility.

Summarizing, based on the observation that the translational mobility of water in these dendrimer-grafted polymer membranes is at most ~40 % of that in the Nafion, we expect that the electro-osmotic dragging would be less in this new membrane.

4. Proton Transport

In these membranes, protons are transported through two different mechanisms: the diffusion of protonated water molecules (vehicular diffusion) and the hopping of the proton along sequences of water molecules (Grothuss diffusion). We calculate vehicular diffusion directly from the MD using $D_{vehicular} = \langle (r(t) - r(0))^2 \rangle / 6t$. However the proton hopping involving forming and breaking covalent bonds as a proton moves from one hydronium molecule to a neighboring water molecule. To study this Grothuss diffusion of proton in water, one must use a method of calculating forces that allows bonds to be formed and broken. This was been done using forces from QM,[32,33] but such QM-MD is limited to ~200 atoms, too few for our studies of hydrated membrane. An alternative is to use the ReaxFF reactive FF, which leads to the same potential barriers for proton hopping as the QM. This is feasible for systems of 1000 to 10000 atoms per cell considered here, but we have not parameterized ReaxFF yet for sulfonic and Teflon system. An alternative approach is the multistate empirical valence bond (MS-EVB) model developed by Voth and coworkers and applied to the proton transport in hydrated membranes.[52-55] Another approach has been used by Paddison and Paul for the self-diffusion coefficient of proton in an arbitrary membrane channel using their non-equilibrium statistical mechanical framework[56-59]

Instead, we employ a simple and efficient method based on transition state theory (TST) to estimate the contribution from proton hopping mechanism to proton diffusion. The QM hopping method has been successfully to investigate the proton hopping in the Dendrion membrane.[12]

To calculate the hopping diffusion in the membrane, we first parameterized the rate constant for the transfer of a proton from the protonated water (hydronium) to the neutral carrier as a function of the intermolecular oxygen in donor and oxygen in acceptor distance (Figure 13a in Reference[12]) using [60,61]

$$k_{ij}(r) = \kappa(T,r)\frac{k_B T}{h}\exp\left(-\frac{E_{ij}(r) - 1/2h\omega(r)}{RT}\right)$$ where $\kappa(T,r)$ and $\omega(r)$ is the tunneling factor and the

frequency for zero point energy correction (given in ref.[60,61]) and E(r) is the energy barrier for the proton to be transferred from donor to acceptor in water medium while they are at a distance of r. We calculated this proton hopping energy barrier for fixed distances between donor and acceptor oxygen in oxygen using QM (B3LYP with the 6-311G** basis) to obtained the energy change as a function of the distance between the proton and the donor oxygen. Then we used the Poisson-Boltzmann self-consistent reaction field model[62,63] to the solvent effect correction along the reaction path and recalculated the energy barrier.

Given the Equation (8), we use the distances between all the pairs of donors and acceptors from the equilibrium molecular dynamics trajectory to calculate the hopping diffusion coefficient as follows:

$$D_{hopping} = \frac{1}{6Nt} \int\limits_0^{t\to\infty} \sum_i^N \sum_j^M k_{ij} r_{ij}^2 P_{ij} dt$$ where N is the number of proton and P_{ij} is the probability

with which a proton can jump from hydronium i to water j defined as $P_{ij} = k_{ij} / \sum\limits_j^M k_{ij}$. Here r_{ij} is the

distance between all the pairs of donors and acceptors measured from the equilibrium molecular dynamics trajectory.

Table 5. Proton diffusion coefficients (D)

Systems (T=353.15 K)		$D_{vehicular}$ (10^{-5} cm^2/s)	$D_{hopping}$ (10^{-5} cm^2/s)	D_{total} (10^{-5} cm^2/s)
PECH-D2	10 wt % water content	0.002	0.300	0.302
	20 wt % water content	0.017	0.379	0.396
PS-D2	10 wt % water content	0.005	0.331	0.336
	20 wt % water content	0.018	0.447	0.465
PTFE-D2	10 wt % water content	0.015	0.440	0.455
	20 wt % water content	0.128	0.563	0.691
Nafion DR=1.1	20 wt % water content	0.290[a]	0.342[b]	0.632[b] (exp. 0.5~0.7)[c]
Nafion DR=0.1	20 wt % water content	0.294[a]	0.407[b]	0.701[b] (exp. 0.5~0.7)[c]
Sulfonic Dendrion	10 wt % water content	0.141[b]	0.377[b]	0.518[b]

a Reference [13]; b Reference [12]; c References [30,64]

Table 5 summarizes the total proton diffusion coefficient ($D_{total} = D_{vehicular} + D_{hopping}$) predicted for all the dendrimer-grafted polymer membranes. We see here that both $D_{vehicular}$ and $D_{hopping}$ increase with increasing water content and the diffusion coefficient increases in order of PECH-D2 < PS-D2 < PTFE-D2 at the same water content. These observations are completely consistent with the above analyses on the structure and dynamics of water in the water phase, suggesting that the water in the membrane approaches that in bulk water as the nanophase-segregation proceeds.

Particularly, the proton diffusion coefficient predicted for PTFE-D2 (0.69 × 10^{-5} cm^2/s) is comparable with that predicted for Dendrion (0.52 × 10^{-5} cm^2/s) and for as Nafion (0.6~0.7 × 10^{-5} cm^2/s. This latter value is in good agreement with the experimental values (0.5~0.7 × 10^{-5} cm^2/s from Zawodzinski[64] and Kreuer[30], Table 4). Considering that PTFE-D2 has the same backbone polymer as Nafion and Dendrion, this result on proton transport confirms that importance of the structure in the water phase of the membrane and the relationship between the nanophase-segregation and the structure and

dynamics in water phase.

5. Summary

This study introduced the concept of a dendrimer-grafted polymer using precisely-defined water-soluble dendritic architecture (sulfonic poly aryl ether dendrimer) in a copolymer with a linear polymer backbone for applications such as PEMFC. In order to investigate the effect of backbone polymer on the properties suitable for PEMFC such as nanophase-segregation and transport, we grafted the second-generation sulfonic poly aryl ether dendrimers onto three different types of linear backbone polymers, e.g. PECH, PS and PTFE for the preparation of three different types of dendrimer-grafted polymer such as PECH-D2, PS-D2 and PTFE-D2.

We found that all these cases the equilibrium systems exhibits nanophase-segregation in which water phase is formed and associated with the hydrophilic dendrimers. Analyzing the pair correlation of sulfur-sulfur in sulfonic acid groups of dendrimers, we found that in the nanophase-segregated structures, the dendrimers contact each other through the membrane, helping the formation of a continuous and percolated water phase.

We also found out that the water coordination number for water molecules in the water phase increases with increasing water content for all cases,. In addition, at the same water content, the water coordination number increases in order of PECH-D2 < PS-D2 < PTFE-D2, indicating that the similarity of the water structure to the bulk water is also in order of PECH-D2 < PS-D2 < PTFE-D2.

The extent of nanophase-segregation in the new copolymer membrane was evaluated quantitatively by analyzing structure factor profiles, S(q) as a function of scattering vector (q) for the membranes with 20 wt % of water content. By determining the characteristic dimension and density contrast in the membrane, we found that the extent of nanophase-segregation increases in order of PECH-D2 (~20 Å) < PS-D2 (~35 Å)) < PTFE-D2 (~40 Å)) which can be compared to 30~50 Å for Nafion and ~30 Å for Dendrion.

We suggest that the structure of the water phase and the structure factor analysis can be understood consistently in terms of the hydrophilicity (or hydrophobicity) of backbone polymer. In comparison to the hydrophilic backbone polymer, PECH, the more hydrophobic PS and the most hydrophobic PTFE have the more extent of nanophase-segregation and thereby achieve the more bulk-water-like structure.

Calculating the rotational diffusion coefficient (D_R) and the translational diffusion coefficient (D_T) from the MD trajectory files, we found that the values of these diffusion coefficients increase with increasing water content, and increase in order of PECH-D2 < PS-D2 < PTFE-D2 at the same water content, indicating that the water dynamics in the hydrated membrane is strongly coupled with the structures in water phase.

We estimated the proton diffusion according to its mechanism: vehicular and hopping. For both mechanisms, the values of proton diffusion coefficients increase with increasing water content, and increase in order of PECH-D2 < PS-D2 < PTFE-D2, which also shows the dependency of proton transport on the structures in water phase as observed in the water dynamics.

Based on the observations from our simulations, we expect that the PTFE-D2 dendrimer-grafted polymer membrane may have comparable performance to Nafion and Dendrion membranes in a PEM fuel cell.

6. Acknowledgement

7. References

(1)   Carrette, L.; Friedrich, K. A.; Stimming, U. *Chem. Phys. Chem* **2000**, *1*, 162-193.

(2) Kreuer, K. D. *J. Membr. Sci.* **2001**, *185*, 29-39.

(3) Paddison, S. J. *Ann. Rev. Mater. Res.* **2003**, *33*, 289-319.

(4) Li, Q.; He, R.; Jensen, J. O.; Bjerrum, N. J. *Chem. Mater.* **2003**, *15*, 4896-4915.

(5) Maurits, K. A.; Moore, R. B. *Chem. Rev.* **2004**, *104*, 4535-4585.

(6) Hickner, M. A.; Pivovar, B. S. *Fuel Cells* **2005**, *5*, 213-229.

(7) Eisenberg, A.; Yeager, H. L., Eds. *Perfluorinated Ionomer Membranes*; American Chemical Society: Washington, D.C., 1982.

(8) Yeager, H. L.; Steck, A. *Anal. Chem.* **1979**, *51*, 862-865.

(9) Yeo, S. C.; Eisenberg, A. *J. Appl. Polym. Sci.* **1977**, *21*, 875-898.

(10) Eisenberg, A.; King, M. In *Polymer Physics*; Stein, R. S., Ed.; Academic Press: New York, 1977.

(11) Scibona, G.; Fabiani, C.; Scuppa, B. *J. Membr. Sci.* **1983**, *16*, 37-50.

(12) Jang, S. S.; Lin, S.-T.; Cagin, T.; Molinero, V.; Goddard_III, W. A. *J. Phys. Chem. B* **2005**, *109*, 10154-10167.

(13) Jang, S. S.; Molinero, V.; Cagin, T.; Goddard_III, W. A. *J. Phys. Chem. B* **2004**, *108*, 3149-3157.

(14) Mayo, S. L.; Olafson, B. D.; Goddard_III, W. A. *J. Phys. Chem.* **1990**, *94*, 8897-8909.

(15) Elliott, J. A.; Hanna, S.; Elliott, A. M. S.; Cooley, G. E. *Phys. Chem. Chem. Phys.* **1999**, *1*, 4855.

(16) Vishnyakov, A.; Neimark, A. V. *J. Phys. Chem. B* **2000**, *104*, 4471-4478.

(17) Vishnyakov, A.; Neimark, A. V. *J. Phys. Chem. B* **2001**, *105*, 7830-7834.

(18) Li, T.; Wlaschin, A.; Balbuena, P. B. *Ind. Eng. Chem. Res.* **2001**, *40*, 4789-4800.

(19) Jang, S. S.; Blanco, M.; Goddard_III, W. A.; Caldwell, G.; Ross, R. B. *Macromolecules* **2003**, *36*, 5331-5341.

(20) Levitt, M.; Hirshberg, M.; Sharon, R.; Laidig, K. E.; Daggett, V. *J. Phys. Chem. B* **1997**, *101*, 5051-5061.

(21) Rappe, A. K.; Goddard_III, W. A. *J. Phys. Chem.* **1991**, *95*, 3358-3363.

(22) Hockney, R. W.; Eastwood, J. W. *Computer simulation using particles*; McGraw-Hill International Book Co.: New York, 1981.

(23) Plimpton, S. J. *J. Comp. Phys.* **1995**, *117*, 1-19.

(24) Plimpton, S. J.; Pollock, R.; Stevens, M. In *the Eighth SIAM Conference on Parallel Processing for Scientific Computing*: Minneapolis, 1997.

(25) Jang, S. S.; Lin, S.-T.; Maiti, P. K.; Blanco, M.; Goddard_III, W. A.; Shuler, P.; Tang, Y. *J. Phys. Chem. B* **2004**, *108*, 12130-12140.

(26) Swope, W. C.; Andersen, H. C.; Berens, P. H.; Wilson, K. R. *J. Chem. Phys.* **1982**, *76*, 637-649.

(27) Agmon, N. *Chem. Phys. Lett.* **1995**, *244*, 456-462.

(28) Agmon, N.; Goldberg, S. Y.; Huppert, D. *J. Mol. Liq.* **1995**, *64*, 161-195.

(29) Kreuer, K. D. *Chem. Mater.* **1996**, *8*, 610-641.

(30) Kreuer, K. D. *Solid state ionics* **1997**, *97*, 1-15.

(31) Kreuer, K. D. *Solid state ionics* **2000**, *136-137*, 149-160.

(32) Tuckerman, M.; Laasonen, K.; Sprik, M.; Parrinello, M. *J. Chem. Phys.* **1995**, *103*, 150-161.

(33) Tuckerman, M.; Laasonen, K.; Sprik, M.; Parrinello, M. *J. Phys. Chem.* **1995**, *99*, 5749-5752.

(34) Tuckerman, M. E.; Marx, D.; Klein, M. L.; Parrinello, M. *Science* **1997**, *275*, 817-820.

(35) Marx, D.; Tuckerman, M. E.; Hutter, J.; Parrinello, M. *Nature* **1999**, *397*, 601-604.

(36) Marx, D.; Tuckerman, M. E.; Parrinello, M. *J. Phys.-Condes. Matter* **2000**, *12*, A153-A159.

(37) Verbrugge, M. W.; Hill, R. F. *J. Electrochem. Soc.* **1990**, *137*, 893-899.

(38) Verbrugge, M. W.; Hill, R. F. *J. Electrochem. Soc.* **1990**, *137*, 3770-3777.

(39) Zawodzinski, T. A.; Neeman, M.; Sillerud, L. O.; Gottesfeld, S. *J. Phys. Chem.* **1991**, *95*, 6040-6044.

(40) Paul, R.; Paddison, S. J. *J. Phys. Chem. B* **2004**, *108*, 13231-13241.

(41) Soper, A. K.; Phillips, M. G. *Chem. Phys.* **1986**, *107*, 47-60.

(42) Farid, A. S. *Platics, Rubber and Composites* **1999**, *28*, 346-356.

(43) Schuster, M.; Kreuer, K. D.; Maier, J. In *14th international conference on solid state ionics*: Monterey, USA, 2003, p 395.

(44) McQuarrie, A. A. *Statistical Mechanics*; Harper & Row: New York, 1976.

(45) Pal, S. K.; Peon, J.; Bagchi, B.; Zewail, A. H. *J. Phys. Chem. B* **2002**, *106*, 12376-12395.

(46) Paddison, S. J.; Reagor, D. W.; Zawodzinski, T. A. *J. Electroanal. Chem.* **1998**, *459*, 91-97.

(47) Paddison, S. J.; Bender, G.; Kreuer, K. D.; Nicoloso, N.; Zawodzinski, T. A. *J. New Mater. Electrochem. Syst.* **2000**, *3*, 291-300.

(48) Mills, R. *J. Phys. Chem.* **1973**, *77*, 685-688.

(49) Krynicki, K.; Green, C. D.; Sawyer, D. W. *Discuss. Faraday Soc.* **1978**, *66*, 199-208.

(50) Price, W. S.; Ide, H.; Arata, Y. *J. Phys. Chem. A* **1999**, *103*, 448-450.

(51) Okada, T.; Xie, G.; Meeg, M. *Electrochim. Acta* **1998**, *14*, 2141-2155.

(52) Lobaugh, J.; Voth, G. A. *J. Chem. Phys.* **1996**, *104*, 2056-2069.

(53) Schmitt, U. W.; Voth, G. A. *J. Phys. Chem. B* **1998**, *102*, 5547-5551.

(54) Schmitt, U. W.; Voth, G. A. *J. Chem. Phys.* **1999**, *111*, 9361-9381.

(55) Petersen, M. K.; Wang, F.; Blake, N. P.; Metiu, H.; Voth, G. A. *J. Phys. Chem. B* **2005**, *109*, 3727-3730.

(56) Paddison, S. J.; Paul, R.; Zawodzinski, T. A. *J. Electrochem. Soc.* **2000**, *147*, 617-626.

(57) Paddison, S. J.; Paul, R.; T. A. Zawodzinski, J. *J. Chem. Phys.* **2001**, *115*, 7753-7761.

(58) Paddison, S. J.; Paul, R.; Kreuer, K.-D. *Phys. Chem. Chem. Phys.* **2002**, *4*, 1151-1157.

(59) Paddison, S. J.; Paul, R. *Phys. Chem. Chem. Phys.* **2002**, *4*, 1158-1163.

(60) Lill, M. A.; Helms, V. *J. Chem. Phys.* **2001**, *114*, 1125-1132.

(61) Lill, M. A.; Helms, V. *J. Chem. Phys.* **2001**, *115*, 7985-7992.

(62) Greeley, B. H.; Russo, T. V.; Mainz, D. T.; Friesner, R. A.; Langlois, J. M.; Goddard_III, W. A.; Donnelly, R. E.; Ringnalda, M. N. *J. Chem. Phys.* **1994**, *101*, 4028-4041.

(63) Marten, B.; Kim, K.; Cortis, C.; Friesner, R. A.; Murphy, R. B.; Ringnalda, M. N.; Sitkoff, D.; Honig, B. *J. Phys. Chem.* **1996**, *100*, 11775-11788.

(64) Zawodzinski, T. A.; Springer, T. E.; Davey, J.; Jestel, R.; Lopez, C.; Valerio, J.; Gottesfeld, S. *Electrochim. Acta* **1995**, *40*, 297-302.